Chapter 5

Ionic Liquid-Based Electrospun Polymer Nanohybrid for Energy Harvesting

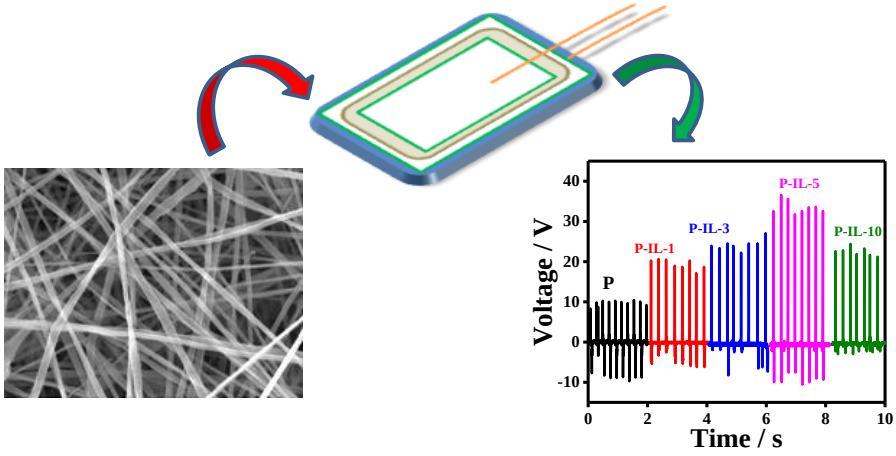

5.1 Introduction

Ionic liquids (ILs) are relatively the new class of materials composed of cations and anions which has grabbed the attention of the researchers due to their unique properties like non-flammability, thermal and chemical stability, high ionic conductivity and almost negligible vapour pressure [161][162]. This functional behaviour of ILs leads them to be used for multifunctional applications. ILs is generally composed of imidazolium, pyrrolidinium, piperidinium or quaternary ammonium cations and organic or inorganic anions [163][164]. The structure and properties of ILs are classified as protic or aprotic, depending on the nature of the ions [162][65]. Polymer based composites in which the polymers are used as matrix is drawing much attraction because of the flexibility, biocompatibility and better mechanical properties of the polymers. Certain nanoparticles are used as fillers with the polymers like graphene, carbon nanotubes, ceramic based fillers, bio-based fillers to attain a specific characteristic which is the combined merits of the polymer and filler.[165][107] ILs also exhibits better interactions with the polymers providing enhanced properties and produce exceptional results in the field of actuators, bio-medical, batteries, metal catalysis, fuel cells, solar cells etc.[100][166] Poly(vinylidene fluoride) (PVDF) and its copolymers have gained much wider recognition in various fields because of their high dipole moment, outstanding electroactive features (like piezoelectric, pyroelectric and ferroelectric behaviour), better mechanical and thermal properties.[167][168] PVDF consists of primarily five different phases α, β, γ, δ and ε phases. α- phase is the common and stable phase having monoclinic unit cell with TGTG' conformation. The β-phase is most significant due to its polar nature and active piezoelectric characteristics. It possesses orthorhombic unit cell with all trans (TTTT) conformation. γ-phase is semi-polar in nature with T_3GT_3G' conformations.[30]-[96] The versatile nature of PVDF makes it most

noteworthy polymer in different fields like medical, fuel cell, energy harvesting etc.[169] [3] Energy harvesting is one such field where PVDF has been the most intriguing polymer due to its remarkable electroactive behaviour. Energy harvesting is the field of study where the waste and unused energies are converted to productive and useful electrical energies. Piezoelectric energy harvesting is the most common one where the various mechanical sources are used to generate considerable energies, effective for small electronic devices [170][129] Several methods are used to generate the electroactive piezo-phases in PVDF, like mechanical stretching or poling or addition of polar piezo-active fillers like bio-waste fillers, ceramic reinforcers, carbon based materials which enhance the polar phase in the polymer [94][171][63][36][98]. There are several instances where ILs is used with PVDF to attain certain properties through change or transform in their crystal structures depending upon the choice of the ionic liquids. Addition of ILs leads to greater interaction between the dipoles of PVDF which in turn helps for the transformation of the non-polar phase to polar phase [172][173][174]. The ability of ILs to transform the non-piezo phase to electroactive phase is one of the many advantages which make it suitable for the piezoelectric energy harvesting applications.

In this work, 1-butyl-3-methylimidazolium chloride (BMIMC) is used as filler incorporated in PVDF matrix to produce electrospun nanofibers. A homogeneous mixture of the PVDF-IL is used for electrospinning at an optimized condition. Solubility of IL in the common solvent of the PVDF leads to better fiber formation. Different concentration of BMIMC is taken to understand the change in the morphology, structure, mechanical, dielectric properties and electromechanical responses. The electrochemical analysis is also evaluated to understand the ionic liquid property within the polymer using different methods. A

device has been fabricated using the electrospun scaffold which is used to observe the impact of IL in the electromechanical behavior for energy generation. Different human movements are applied to produce considerable energy output from the fabricated device.

5.2 Experimental

The processing details and materials are stated in chapter 2.

5.2.1 Electrospun nanohybrid preparation*:* The prepared solution was transferred to a syringe of 0.8 mm diameter and electrospun over an aluminium foil as substrate at 21 kV, at an injection rate of 0.5 ml/hr. 10 % w/v and 15 cm distance between the drum collector and the spinneret was maintained. IL was used at different concentrations w.r.t. the polymer weight and was abbreviated as P, P-IL-1, P-IL-3, P-IL-5, and P-IL-10 for 0, 1, 3, 5 and 10 wt. % IL concentration, respectively.

5.3 Characterization

Some of the characterization techniques used is discussed in chapter 2.

The electrochemical analysis is performed using the Autolab M204 with a frequency response analyzer (FRA32) at room temperature. The membrane is placed between the lab prepared electrodes (grade 5 materials) with a circular dimension. Cyclic voltammetry (CV) is performed with a scan rate of 100 mV/s within the range of ± 1V as applied potential. Ionic conductivity is measured across the electrode using the sinusoidal AC frequency response in the range of 0.1 to 10^6 Hz. The wire resistance is eliminated by performing the blank spectrum. The ionic resistance is measured using the simulation and fit process using the software. The ionic conductivity (σ_i) is calculated using the following equation:

$$\sigma_i = d / (R_i \times A) \quad (1)$$

where, d is the thickness of the active material, A is the area and R_i is the resistance. The Bode modulus and Bode phase is measure in accordance with the impedance analysis.

5.4 Results and Discussion

The addition of ILs to polymeric matrix of PVDF leads to substantial changes in the morphology of the electrospun fibers. The optical microscopic images (***Figure 5.1a***) suggest that addition of ionic liquids leads to the reduction of the beads formation in the PVDF-IL composites as compared the pristine PVDF. The reduction of beads and thinner fiber formation can be well viewed from the higher magnification images obtained from SEM (***Figure 5.1b*)**. Thus, the incorporation of IL to the polymer results in better fiber formation which can be attributed to better dispersion due to the conducting nature of IL provided to the PVDF matrix along with greater dipolar interaction which exhibit in the combined effort of the stretching and poling during electrospinning thereby leading to formation of fine fiber. Along with the good fiber formation, the size of the fiber gets reduced as compared to the pure PVDF fiber. ***Figure 5.1c*** and ***5.1d*** represents the fiber diameter distribution and the average fiber diameter obtained from the SEM morphology. From the distribution curve, it can be seen that there is a wide distribution of the fiber at different dimensions but incorporation of the IL narrow down the distribution of the fiber diameter. The average fiber diameter obtained for P, P-IL-1, P-IL-3, P-IL-5 and P-IL-10 are 241 ± 12 nm, 193 ± 9.5 nm, 181± 9 nm, 148 ± 7 nm and 230 ± 11 nm, respectively. It can be seen that the fiber diameter reduces till 5 wt. % concentration of IL while the diameter increases at 10 wt. % of IL concentration.

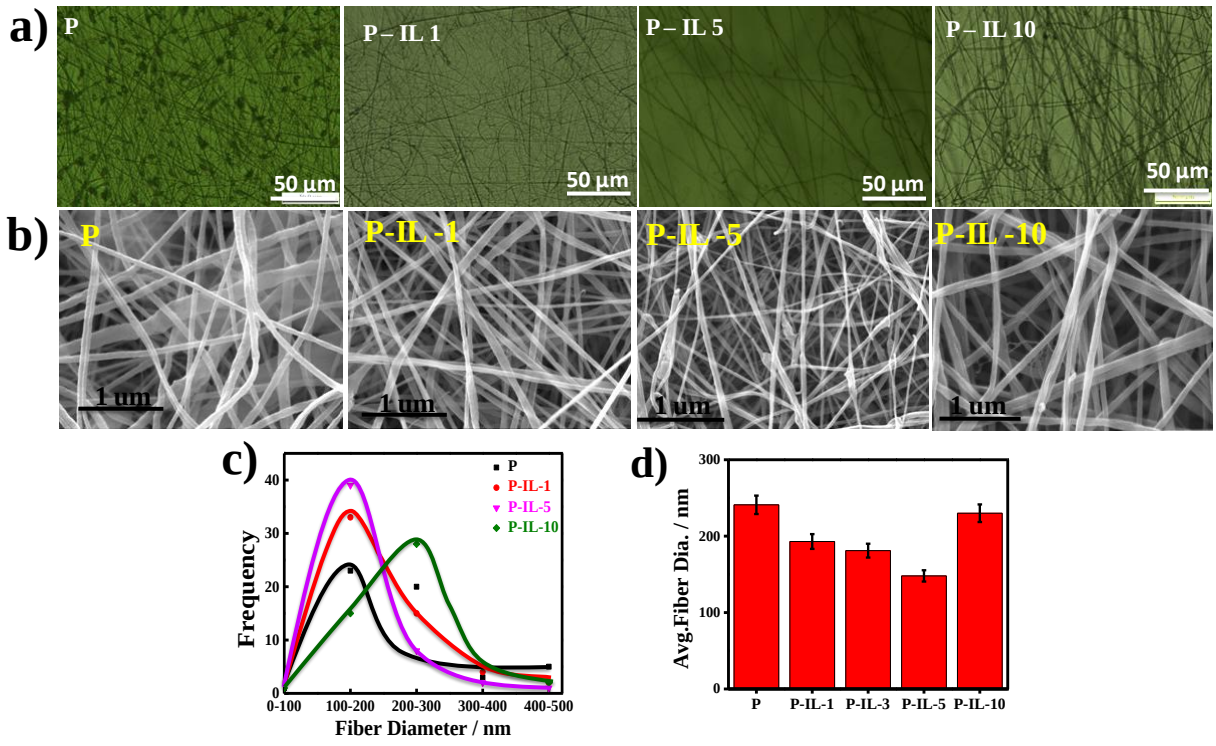

Figure 5.1: **a)** Optical images for the electrospun nanofibers (P, P-IL-1, P-IL-5 AND P-IL-10); **b)** SEM images of fibers for pristine PVDF and its indicated hybrids; **c)** fiber diameter distribution for the electrospun scaffolds; and **d)** average fiber diameter for the indicated nanofibers

The increasing dimension at higher IL concentration might be due to the increase in viscosity of the P-IL solution at higher IL concentration. However, ionic liquid helps in the formation of good quality of fiber with narrow distribution. The morphological variations due to the incorporation of IL make it urgent to investigate the structural alterations due to the addition of IL in the PVDF matrix. X-ray diffraction (XRD) pattern in ***Figure 5.2a*** indicates the structural changes with the different content of IL in PVDF. For neat PVDF, there can be seen two peaks at 18.5° (020) which correspond to the α-phase while the major crystalline peak at 20.4° (110 / 020) is for the β-phase [96].

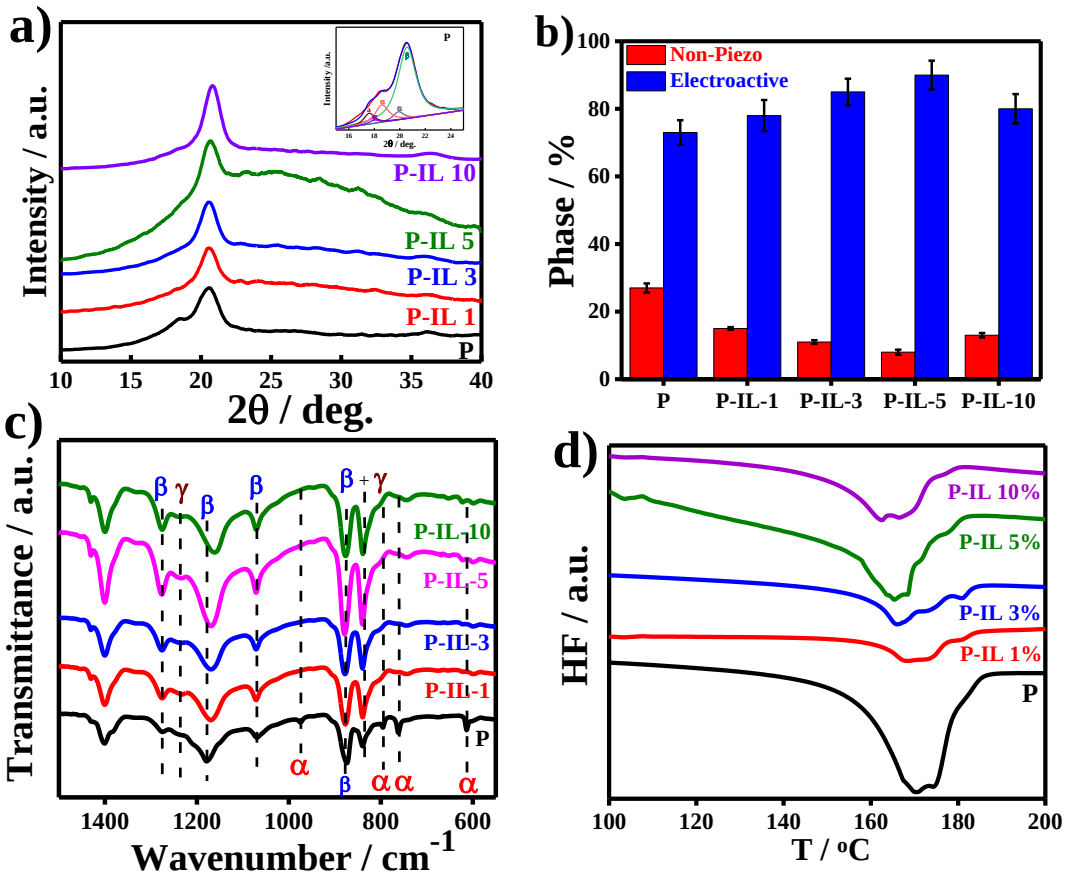

Figure 5.2: a) XRD patterns for the prepared nanofibers (inset shows the deconvolated peaks); **b)** estimated phase fraction from the deconvolated peaks of the electrospun hybrids and neat PVDF; **c)** FTIR spectra representing the different phases formed; and **d)** DSC curves for the pristine polymer and its indicated hybrids.

Pristine PVDF generally consists of α-phase but possess the ability to get transformed to the electroactive phase using some processing methods like stretching or poling and addition of electroactive fillers which reinforces the polar phase to the polymer and the conformation changes from TGTG' (α-phase) to TTTT (β-phase). Addition of the IL to the PVDF matrix promotes better electrostatic interaction between the positive part of the PVDF and the negative part of the IL (anion), developing a dipole moment in the system,

which in turn enhances the electroactive phase formation. However, the appearance of α-phase is explained from the bead formation in pure PVDF after electrospinning. Addition of ILs to the PVDF matrix leads to shifting of the crystalline β peak to 20.5^{o} and 20.6^{o} for P-IL-3 and P-IL-5, respectively. More importantly, the diminishing of the non-polar α–phase peak indicates that the addition of the IL leads to nucleation of β-phase which results in transformation of the non-piezo phase to the piezo-active phases. In case of P-IL-5, broadness is seen around 25.4° (120 / 021) which can be due to the development of the semi-polar γ-phase [94][175][176]. There have been some evidences in some previous works where IL addition to the polymer matrix leads to development of the electroactive phases and the results obtained here support the generation of polar phase due to incorporation of the ILs [173][176]. To quantify the development of the electroactive phases for PVDF and its hybrids, the XRD peaks are deconvolated as shown in the inset of the ***Figure 5.2a***. ***Figure 5.2b*** represents the phase fraction of the non-polar and electroactive phases produced in the fibers of different samples. For pristine PVDF, the amount of electroactive phase is around 73% which increases to almost 90% in case of the P-IL-5. Thus, the rise in the electroactive phases supports that the addition of IL into polymer leads to transformation of the non-polar phase to piezo-active phase as evident from the XRD patterns. Further, the electroactive phase fraction gets reduced to around 80% for higher content of IL in P-IL-10. The reduction of the polar phase for higher IL content might be due to the viscous nature of the polymer–IL solution, which causes aggregation. The effect of ILs on the PVDF is also confirmed through the FTIR-ATR spectra (***Figure 5.2c***). The peaks at 610, 761, 797 and 975 cm^{-1} correspond to the α-phase for pristine PVDF while the β-peaks are seen at 876, 1070, 1176 and 1275 cm^{-1}. The peak

at 1235 cm^{-1} represents the γ-phase while the peak at 838 cm^{-1} is the combination of both β and γ phases. Similar peaks have been reported in the literature for PVDF based systems [96]. However, incorporation of ILs in PVDF leads to the diminishing or almost disappearance of the α-phase peaks. The peaks get shifted in case of the β-peaks with the increase in IL content indicating the better interaction of IL with the PVDF matrix. Hence, it is obvious from the spectra that the ILs leads to the nucleation of the electroactive phases which can be observed from the rise in intensity of the polar phase peaks of the nanofibers. ***Figure 5.2d*** shows the changes in the melting temperature (T_m) of the electrospun hybrids with different IL content. The neat PVDF fiber shows two peaks at 170° and 174 °C which are the melting peaks for β and α–phases, respectively. With the addition of IL in the polymer, the melting temperatures for the β –phase shifts toward the lower temperature, 168°, 166° and 165 °C for P-IL-1, P-IL-3 and P-IL-5, respectively. The lowering of T_m with the rise in IL content can be attributed to the better miscibility of IL and greater interaction with the polymer, which resulted in better fiber formation as evident from the SEM images. The melting peak for the α–phase gets broaden and has reduced with the IL incorporation. As evident from the XRD and FTIR studies, the rise of γ-phase is also observed in the DSC curves with the increasing content of the IL in the polymer. For P-IL-1, the melting temperature of the γ-phase is seen at 181 °C which further shifts to 179 °C for P-IL-5 and the peak is slightly reduced in P-IL-10. This is to mention that the order of the melting temperature for the different phases of the PVDF follows the order β<α<γ [93]. From the DSC thermograms, it is evident that the addition of the IL induces the piezoelectric crystalline phase in PVDF because of the electrostatic interactions developed between IL and PVDF which leads to the reduction of the T_m on increasing the addition of

the IL [174][175][176]. Hence, better interaction between IL and PVDF leads to the enhancement of the electroactive phases which supports the results drawn from the XRD and FTIR spectral studies.

The mechanical stability of the material is the important parameter which supports its ability to be used for various applications including devices. The mechanical properties of the prepared electrospun scaffold is analysed using the tensile stress-strain measurement performed at room temperature as shown in ***Figure 5.3a.*** From the stress-strain curve it is apparent that the addition of IL to PVDF matrix increases its mechanical strength upto certain IL loading after which the properties get reduced. The histograms in ***Figure 5.3b,c*** represent the modulus and toughness of the neat PVDF and its hybrid with varying IL content. The modulus is calculated using the linear part of the curve while the toughness is measured by the area under the stress-strain curve. The modulus for pure PVDF is around 3.8 ± 0.14 MPa which increase to 70 ± 3.2 MPa for P-IL-5 but gets reduced to 39 ± 1.9 MPa in P-IL-10. The increase in the modulus and toughness with IL loading can be correlated to the thinning and flawless fibers as seen from the SEM images which are due to the better dispersion of the IL in the polymer environment. With the rise in IL content after certain concentration, the mechanical properties reduce which may be attributed to the rise in plasticizing effect of the IL within the PVDF matrix [177][173][47].

The dielectric relaxation behavior of the electrospun fibers is analyzed in ***Figure 5.3 d-h***. The frequency dependent dielectric permittivity (ε') and dielectric constant (ε_r) of PVDF and its hybrids with varying IL content is explored in ***Figure 5.3d-e,*** respectively. It is obvious from the curves that the dielectric parameters tend to have an increasing trend with the rise in IL content as compared to neat PVDF.

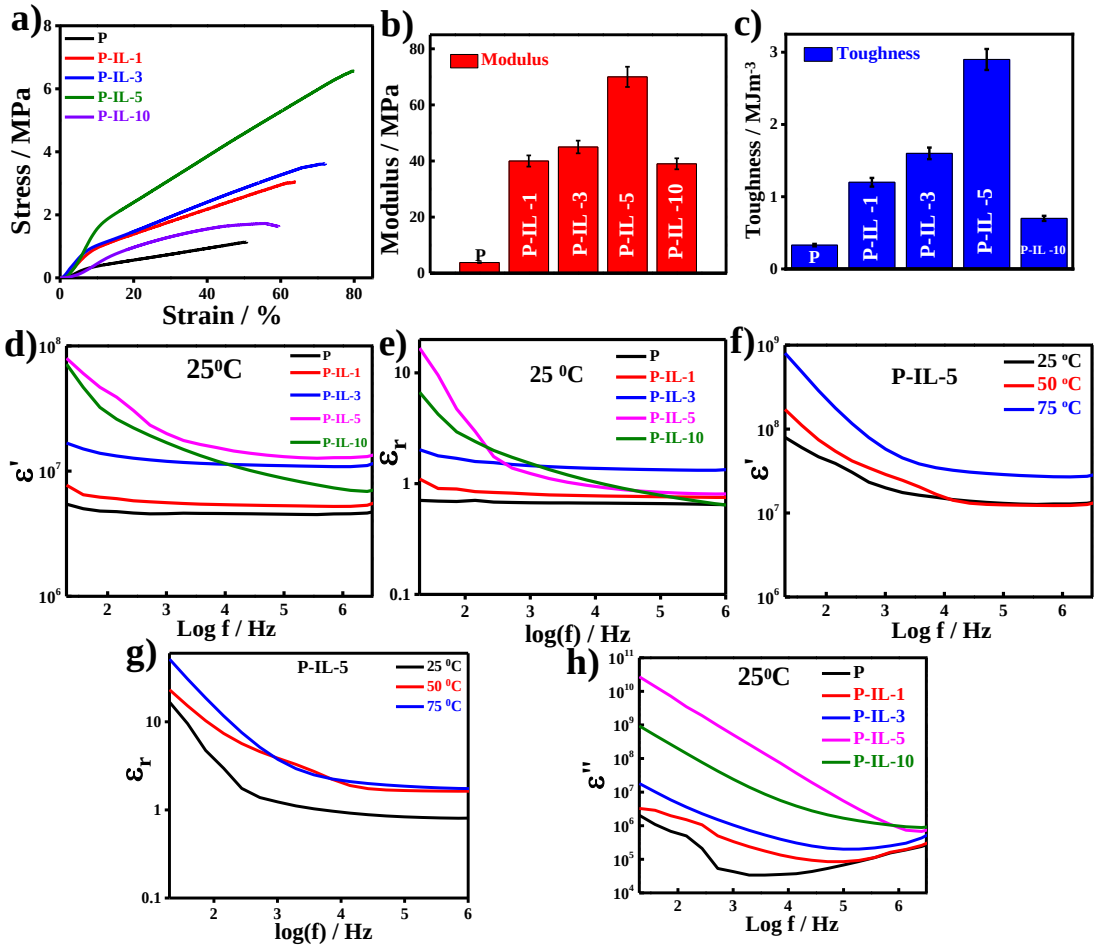

Figure 5.3: a) Stress-strain curves for the prepared nanofibers; b) calculated modulus for the nanofibers from the stress – strain curves; c) toughness derived from the tensile test of the prepared scaffolds; d) dielectric permittivity as a function of frequency for the pristine polymer and its nanohybrids as indicated; e) dielectric constant as a function of frequency at room temperature; f) and g) dielectric permittivity and dielectric constant at different temperatures for P-IL-5 nanofiber and h) dielectric permittivity (imaginary) for the pristine polymer and its nanohybrid at 25^0C.

The maximum dielectric constant for PVDF is around 0.8 while the P-IL-5 has the value around 16.7. The rise in the dielectric values can be credited to the better ion transport and

decoupling of IL which leads to maximum number of charge carriers into the polymer matrix [178]. It is also evident from the curves that at higher frequencies the dielectric parameters get invariant and the values almost get stabilized. The dielectric relaxation phenomenon comprises of the alignment of the polarization in PVDF which is due to the rotational motion of the $–CF_2$ moiety. At a higher frequency the rotational motion of the $–CF_2$ dipole is unable to attain the equilibrium with the applied field as a result the ε' and ε_r get reduced and level off with increasing frequency. This invariant behavior of the hybrids at the higher frequency is reported in some literatures [173]. ***Figure 5.3 f-g*** represent the temperature dependence of the ε' and ε_r at different temperature for P-IL-5 nanofiber, respectively. The imaginary dielectric permittivity (ε") for PVDF and its nanohybrid and the variations in the parameter at room temperature is shown in ***Figure 5.3h***. It is evident that the ε' and ε_r values get increased with the rise in temperature. The rise in the dielectric values with the temperature is due to the various contributions such as electrode polarization, dc conductivity, Maxwell-Wagner relaxation and charge and motion transport. [179][169].

The effect of the ILs on the electrochemical properties is analyzed in the ***Figure 5.4***. The addition of ionic liquid to polymer matrix benefits its ionic mobility and thus should enhance its ionic transport mechanism. ***Figure 5.4a*** shows the cyclic voltammetric (CV) study of the prepared electrospun scaffold. The increase in the content of IL enhances the output current against the applied potential. The rise in current is due to better mobility of the ionic liquid through the polymer which leads to an order higher in magnitude of the output current in P-IL-10 than the pristine polymer. The ionic conducting capability of the

nanofibers is analysed using the electrochemical impedance spectroscopy (EIS) in the ***Figure 5.4b***.

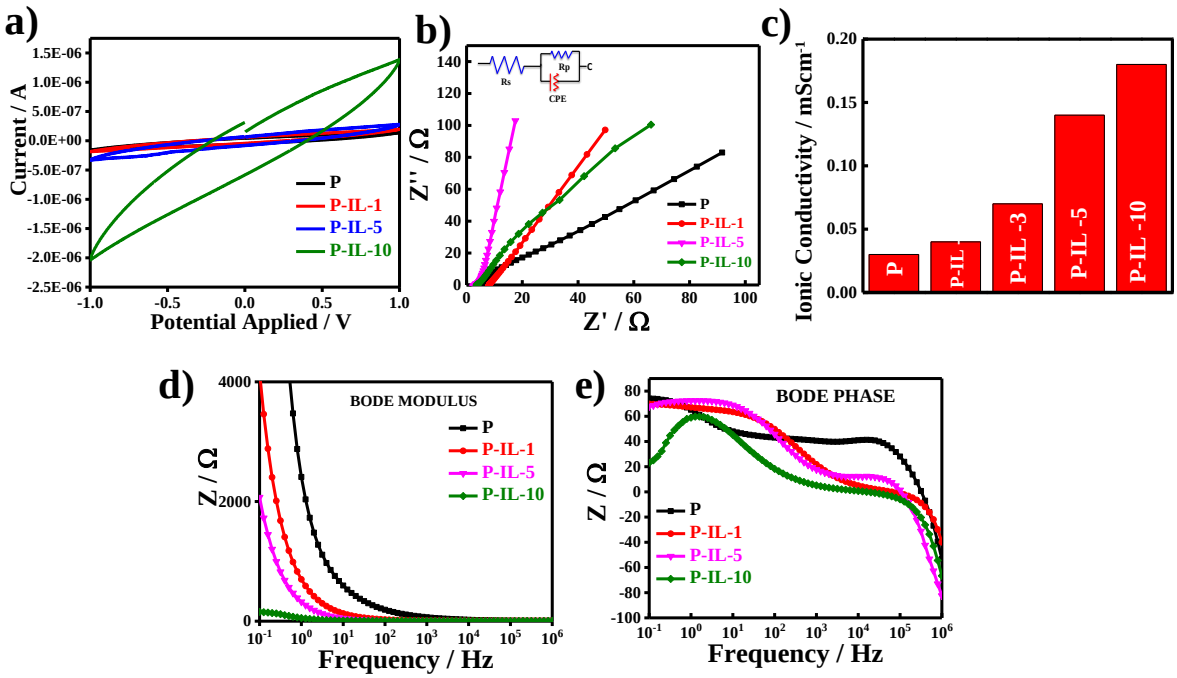

Figure 5.4: a) Cyclic voltammetry of the prepared nanofibers at 100 mV / s; b) Nyquist plot for the nanofibers (equivalent circuit has been shown in the inset); c) ionic conductivity, measured from the Nyquist plot, of the indicated scaffolds; d) Bode modulus as a function of frequency for the pristine polymer and its indicated hybrids; and e) Bode phase as a function of frequency for the electrospun scaffolds.

The Nyquist plot between the real and imaginary impedance corresponds to the addition of IL leading to better ionic transport and the ionic resistance is measured using the simulation and fit method. The resistance tends to reduce with the IL incorporation. The equivalent circuit for the measurement is presented in the inset of ***Figure 5.4b***. The nature of the Nyquist plot is almost linear due to the lower conductivity of the polymer. The ionic conductivity is calculated and found to be of increasing trend with rise in IL concentration.

The measured ionic conductivities are 0.03, 0.04, 0.07, 0.13 and 0.18 mS/cm for P, P-IL-1, P-IL-3, P-IL-5 and P-IL-10, respectively, as shown using bar diagram in ***Figure 5.4c***. The ionic conductivity systematically increases with the increase in IL content due to the better ion transport and dispersion of IL in polar PVDF matrix. The better ionic conductivity is due to the dual contribution of the anions and cations of the IL. The Bode modulus and Bode phase is also performed to support the observations from the Nyquist plots. ***Figure 5.4d*** exhibits the Bode modulus (impedance as function of frequency) which suggests that the impedance decreases as the frequency is raised irrespective of IL content which is due to the localized dynamics of the ionic mobility. At higher content of the IL (10 wt. %), the impedance is lower than pristine polymer which may be due to the higher charged carrier numbers and their ion transport. Similarly, the Bode phase (phase angle as a function of frequency) in ***Figure 5.4e*** suggests that the increase in IL loading reduces the phase angle as compared to pure polymer fiber. This behaviour is due to the polarization relaxation phenomenon which depends on the ionic liquid content [180][181].

Now, it is pertinent to analyse the energy harvesting properties of the fabricated device using the electrospun scaffolds. The results from the morphological, structural and mechanical analyses suggest that the developed material has all the merits to be used for the piezoelectric energy harvesting applications. Incorporation of IL to the PVDF enhances the electroactive phase which induces the piezoelectricity in the material that can be used to harvest energy from the waste mechanical energies to beneficial electrical output. ***Figure 5.5a*** depicts the schematic representation of the fabricated device prepared from the electrospun fibers of PVDF and IL. The device is designed using aluminium sheet acting as substrate for the electrospun fibers, copper wires as electroding material and PDMS as the

encapsulated material to provide the rigidity and stability to the device. The piezoelectric coefficient (d_{33}) measured across the material at room temperature is presented in the ***Figure 5.5b***. The d_{33} value for the neat PVDF scaffold is -5 pC/N which increases to -17 pC/N for P-IL-5. The rise in the d_{33} value with the IL loading attributes to the better fiber generation in the presence of conductive fillers which leads to higher electrostatic interactions between the IL moieties with the PVDF arising from better dipole alignment. As observed from the other characterizations, the behaviour of the nanohybrid at higher IL loading (10 wt. %) gets reduced which is clearly evident from the decrease in d_{33} value -11 pC/N for P-IL-10. The designed device is further used to analyse its ability to harness energy from different motions of the human body. The material is subjected to external pressure from different human body parts like finger and leg and its electromechanical response is measured. The frequency applied over the device is around 4 Hz (almost 4 hits per second). ***Figure 5.5c*** shows the output voltage generated from the finger tapping against the device at different IL loading in PVDF matrix. The maximum output voltage (peak-to-peak) for pristine PVDF fibre through finger tapping mode is around 20.8 V which increase to 27.6, 35.5, 48 and 28.5 V for P-IL-1, P-IL-3, P-IL-5 and P-IL-10, respectively. There is a systematic increase in output voltage up to 5 wt. % content hybrid nanofiber device. The drop in the output voltage after 5 wt. % loading of the IL corresponds to the drift in the electroactive phase content due to agglomeration or improper dispersion of IL at higher content as observed from the other characterizations.

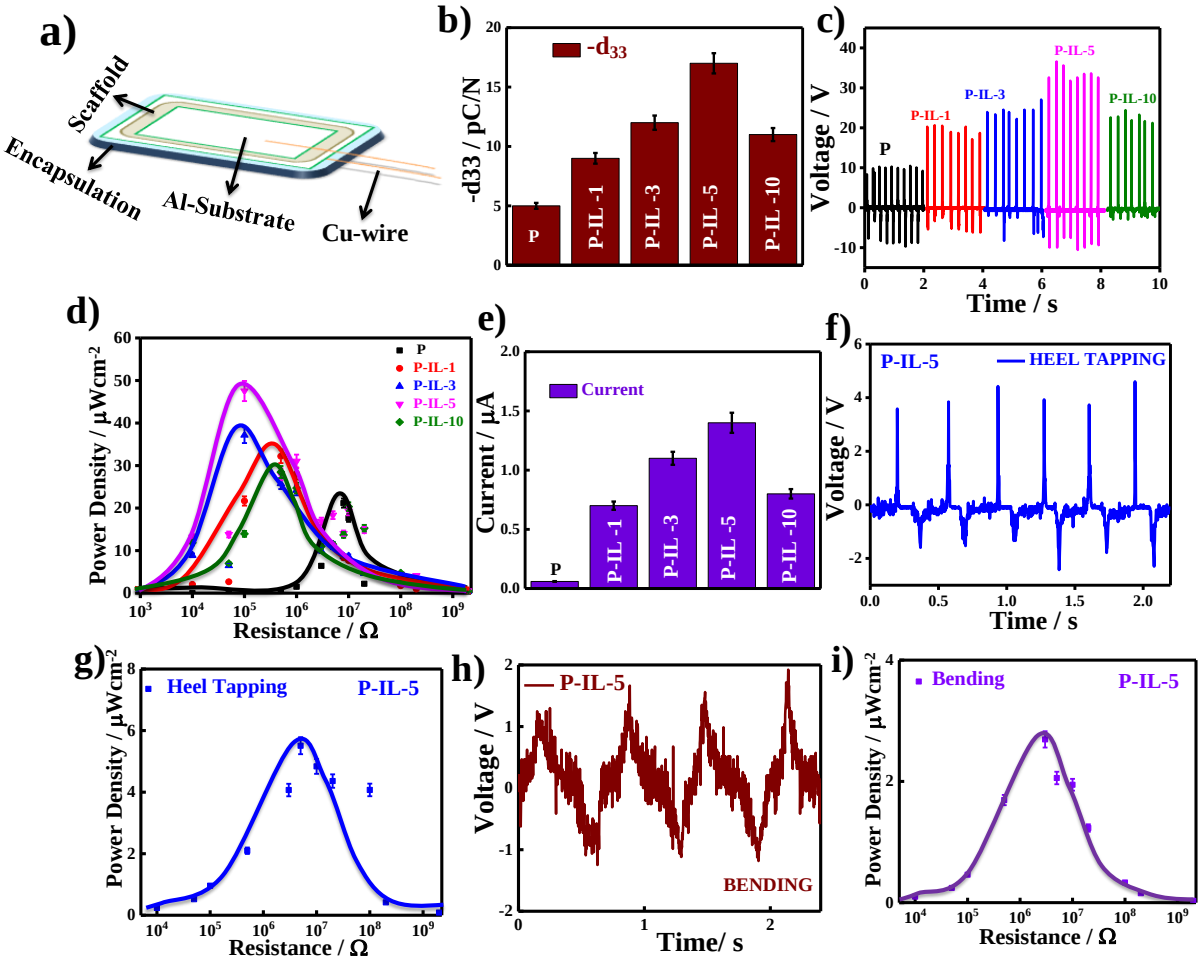

Figure 5.5: a) Schematic view of the fabricated device; b) piezoelectric coefficient (d33) values in the form of bar diagram for the indicated nanofibers scaffold; c) output voltage generated from the device using finger tapping mode using the indicated scaffolds; d) power density curves as a function of resistance for the pristine polymer and its hybrids as indicated; e) measured output current from the indicated devices; f) and g) output voltage and power density produced from the heel tapping mode for the representative P-IL-5 device; h) and i) measured output voltage and power density obtained through bending mode on the P-IL-5 nanofiber based device.

The estimated stress applied through finger tapping is found to be around 32 kPa as reported in the literatures [61]. The calculation for the applied stress is demonstrated as below:

When the finger or the object impacts the developed device, the pressure applied on the object results in the charge generation. Built on the kinetic energy and momentum theorem, the applied stress is calculated using the following equation:

$$m.g.h = \frac{1}{2}mv^2 \tag{5.1}$$

$$(F - m.g).\Delta t = m.v \tag{5.2}$$

$$\Delta\sigma = \frac{F}{A} \tag{5.3}$$

Where m is the mass of the finger or object, g is the acceleration due to gravity, h is the dropping height of the object, v is the velocity, $\Delta\sigma$ is the applied stress, A is the surface area of the device, F is the applied force of contact and Δt is the time span between two impacts.

The approximate values of the variables required for stress calculation is m ~ 0.45 kg; A~ 405 mm^2; Δt ~ 0.06 sec; h ~ 0.065 m and g = 9.80 N/Kg.

Estimated Force (F) ~ 12.88 N and hence the Stress applied ($\Delta\sigma$) ~ 32 KPa.

The mechanism of the piezoelectric material to generate substantial electrical output on the application of external pressure is presented in several previous articles. On the application of the external pressure on the material, electrical charge generates between the electrodes which moves back and forth leading to the production of the electrical signal in the external

circuit. The induced polarization due to the mechanical strain in the device develops a potential difference between the both ends of the device. The developed potential causes the flow of electrons from the electrode to the external load which in turn balances the electric field and gives a positive signal. The charge generated moves back to the electrode resulting in the negative signal when the load is removed or released [29][158][124].

The device is subjected to the external resistance and power density (P_d) has been calculated using the following formula;

$$\mathbf{P_d = V^2 / (R \times A)} \qquad (5.4)$$

where, R is the resistance applied across the device, V is the output voltage produced and A is the area of the active material across which load is applied.

The power density obtained for different loading of the IL is presented in the ***Figure 5.5d***. The power density obtained for pure PVDF fibre is around 21.2 μWcm^{-2} which rises to the 47 μWcm^{-2} for P-IL-5 with gradual increase with IL content in the scaffold fibers. The increase in the power density with the IL loading can be attributed to the greater electroactive phase generation and better interaction with IL with PVDF matrix. The better quality of the fibers and improved alignment leads to greater electrostatic interactions arising from the conductive nature of the ionic liquids. The device is then subjected to the measure of the output current generated from the finger tapping motion using the digital multimeter as shown in ***Figure 5.5e***. Maximum output current obtained is around 1.4 µA for P-IL-5 as compared to the 0.06 µA for pristine PVDF. Addition of the IL increases the current as compared to PVDF fibre based device which is the conclusive effect obtained from the structural analysis of the electrospun scaffold with IL variations. Different motions of the human body are being used to observe the electromechanical responses of

the device. ***Figure 5.5f and 5.5g*** shows the maximum output voltage (peak-to-peak) and power density obtained through heel tapping. The device generated around 7.1V (peak-to-peak) of maximum output potential and power density of 5.5 μWcm^{-2}. Bending of the device produced around 3.2 V and 2.7 μWcm^{-2} of maximum output voltage (peak-to-peak) and power density respectively as seen in ***Figure 5.5h and 5.5i***. The application of the external stress over the device generates no cracks or deformation in the overall device which explains the stability and uniformity of the fabricated device. Though the output generated using the heel tapping and bending is considerably less which is due to the impact applied by the external pressure on the device still the output measured is better and implies the ability of the device to harness energy from different human body motions. When an external pressure is applied to the nanogenerator, its crystal structure gets distorted which leads to the generation of electromechanical response through the movement of charges across the electrodes. The alignment of dipoles changes under the application of stress resulting in the net dipole moment in the system. However, human body movements are used to impart external stress to the device causing the charges to generate across the electrodes of the nanogenerator and the mechanism of the press and release develops a potential difference which is measured as output signal. Under a constant stress, no charge is generated or produced and thereby, no output signal is obtained.[127][97] Hence, the efficacy of the device is conclusive that incorporation of the IL in the PVDF matrix enhances the electroactive polar phases which induce better piezoelectric application of the fabricated device against variant external pressure.

5.5 Conclusions

IL-based PVDF nanofibers are prepared using the electrospinning process at varying IL concentrations. The IL is added as a reinforcing agent to the polymer matrix which leads to better fiber generation than the pristine PVDF fiber. The average fiber diameter decreases with the IL loading but after certain concentration of the IL loading the fiber diameter start increasing due to the rise in viscosity of the solution that leads to thicker fibers. The addition of IL raises the electroactive phase content up to ~90% as compared to 73% for neat PVDF fibers. The transformation of the non-polar phase to piezo active polar phase is evident from the XRD, FTIR and DSC studies which support the development of the consolidated fibers on IL addition to the PVDF. The mechanical properties tend to rise up to 5 wt. % of the IL loading as compared to pure PVDF fiber which is significant enough to use the electrospun fibers for device based application due to its better strength and flexibility. Dielectric relaxation analysis supports the observation from other tests that IL incorporation enhances the material efficiency and the dielectric parameters increases with the increase in the temperature. The electrochemical study reveals that addition of IL leads to better ion transport and higher carriers which results in increase in ionic conductivity. Higher IL content nanofiber shows maximum ionic conductivity of 0.18 mS/cm as compared to 0.03 mS/cm for pristine PVDF. The electrospun fiber is utilized to design a device which is used to measure the electromechanical responses through different human body movements. Finger tapping generated a maximum output voltage (peak-to-peak) of 20.8 V and 48 V for P and P-IL-5, respectively. Power density is calculated across the variable resistance load and the maximum power density obtained is around 47 μWcm^{-2} as compared to the 21.2 μWcm^{-2} for pure PVDF fiber. Heel tapping and bending modes also generate considerable amount of output voltage and power which clarify the ability of the

material to harness energy from small impact or pressure. The efficacy of the device and material is well determined and concludes the ability of the material to be a potential material for energy harvesting.